

promote angiogenesis, tumor growth, and metastasis in murine carcinoma models (19–23), including ovarian carcinoma (24). Our recent data suggest that chronic stress is associated with increased IL8 levels. However, the exact mechanism of IL8 induction is not fully known. Here, we describe an ADRB2- and FosB-mediated increase in IL8 that provides a new understanding of stress-driven tumor growth.

EXPERIMENTAL PROCEDURES

Cell Lines and Culture Conditions—The HeyA8 and SKOV3ip1 ovarian cancer cell lines were propagated as described previously (25). Briefly, HeyA8 and SKOV3ip1 cell lines were maintained in RPMI 1640 medium that was supplemented with 10% fetal bovine serum (FBS) and 0.1% gentamicin sulfate (Gemini BioProducts, Calabasas, CA) in 5% CO₂, 95% air at 37 °C.

Analysis of IL8 Expression in Response to NE and Epi Treatment—Real time RT-PCR was performed to assess IL8 mRNA expression in ovarian cancer cells (HeyA8 and SKOV3ip1) after treatment with increasing doses of NE and Epi using the RNAqueous kit (Ambion) following the manufacturer’s protocols. For blocking experiments, cells were pretreated with propranolol (10 μM) for 3 h prior to the addition of NE or Epi. Cells were then washed twice with D-PBS and placed in –80 °C for at least 20 min. mirVana kit (Ambion) was then used for RNA extraction according to the manufacturer’s guidelines. The mRNA was then transcribed into cDNA. PCR amplification was performed on cDNA following the conditions and primers described previously (24). The cDNA was resolved on 2% agarose gels and quantified using Foto/Analyst Luminary software (Fotodyne, Hartland, WI).

Enzyme-linked Immunosorbent Assay (ELISA)—IL8 protein levels in the supernatant collected from cells treated with either NE or Epi were quantified by ELISA, using the Quantikine Immunoassay kit (R & D Systems, Minneapolis, MN) according to the manufacturer’s protocol and as described previously (24). Additionally, to determine the specific AP1 complex component activated by NE, SKOV3ip1 cells were treated with 10 μM NE for 5 min. Nuclear extracts were prepared and probed for specific AP1 family members by ELISA (TransAM AP1-Family Transcription Factor Assay, Active Motif, Carlsbad, CA) as described above. Samples were assayed in duplicate, and data represent the mean fold induction over triplicate experiments.

IL8 Promoter Analysis—HeyA8 or SKOV3ip1 (3 × 10⁵) cells were transfected (Lipofectamine 2000; Invitrogen) with a full-length sequence (26, 27) of IL8 promoter (1481 bp upstream of transcription start site) and subsequently assayed for luciferase reporter gene expression (Promega) after 3 h of exposure to vehicle control or pharmacological agonists/antagonists of β-adrenergic receptors or PKA. All analyses were carried out in triplicate, and results were compared with those from a truncated promoter sequence (133-bp upstream sequence), and sequences in which AP1, NF-κB, or CCAAT/enhancer-binding protein (C/EBP) (NFIL6) motifs were disrupted by site-directed mutagenesis.

Electrophoretic Mobility Shift Assay (EMSA)—HeyA8 ovarian cancer cells were exposed to NE for 15 min, after which nuclear proteins were isolated (CellLytic NuCLEAR, Sigma)

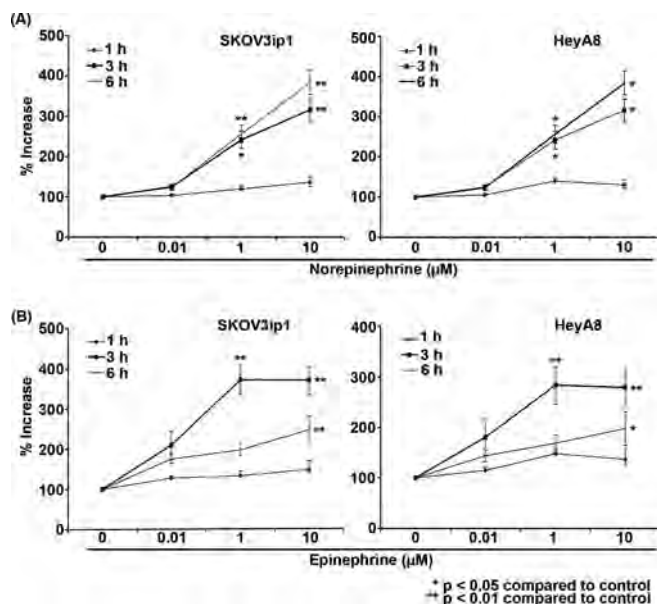


FIGURE 1. **Effects of NE or Epi on IL8 protein levels.** IL8 levels were assessed by ELISA in SKOV3ip1 and HeyA8 ovarian carcinoma cells after 1, 3, and 6 h of exposure to NE (A) or Epi (B). Average percent increase in IL8 levels compared with controls is reported. Error bars represent S.E.

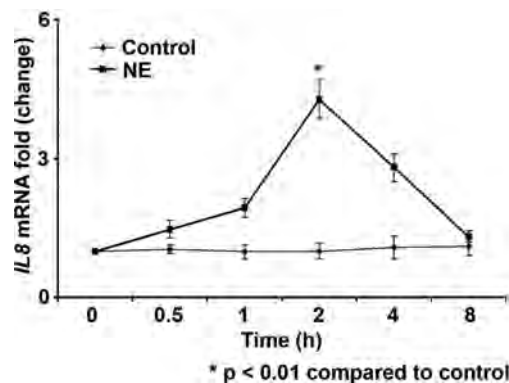


FIGURE 2. **Effect of NE on IL8 mRNA levels.** IL8 mRNA levels were determined by real time RT-PCR in SKOV3ip1 ovarian cancer cells after exposure to NE (10 μM) at different time points. Average fold change in IL8 mRNA compared with control is reported. Error bars represent S.E.

and probed for AP1 or Sp1 activation using Cy5-tagged double-stranded oligonucleotides bearing consensus transcription factor-binding motifs (Operon) as follows: Sp1 (Cy5)-5’-ATT-CGATCGGGGCGGGGCGAGC-3’; AP1 (Cy5)-5’-TTCCGG-CTGAGTCATCAAGCG-3’. Transcription factor-bound oligonucleotides were resolved by electrophoresis through a 5% acrylamide gel for 90 min at 200 V, followed by fluorescence imaging on a Typhoon 9410 system (GE Healthcare).

Invasion and Migration Assays—The effects of IL8 gene silencing on SKOV3ip1 cell invasion and migration were analyzed using membrane invasion culture system as described previously (24). Briefly, SKOV3ip1 cells were transfected with IL8 or control siRNA. Twenty four hours later, 1 × 10⁵ cells were resuspended in 100 μl of serum-free media and added to upper wells. A 0.1% gelatin (migration) or defined matrix (invasion)-coated membrane separated the upper and lower wells. Lower wells contained 5% serum-containing media. The culture system was incubated (migration, 6 h; invasion, 24 h) at

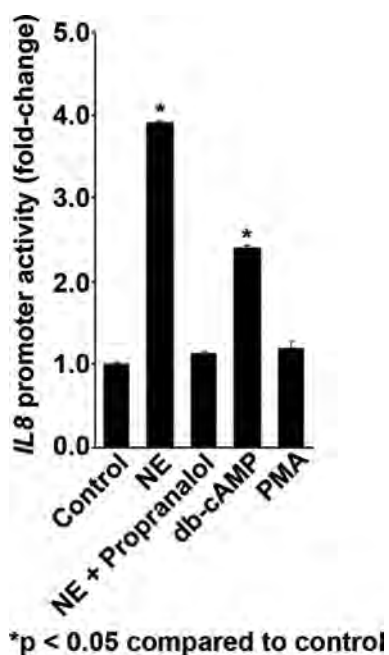


FIGURE 3. **NE transcriptional control of the IL8 promoter.** IL8 promoter activity was assayed by expression of a luciferase reporter gene in HeyA8 ovarian cancer cells after 3 h of exposure to NE (10 μ M). The role of β -adrenergic signaling was evaluated by pretreatment of NE-exposed cells with the β -blocker propranolol. The role of PKA activity was assessed by pharmacological activation by Bt₂cAMP (*db-cAMP*) (100 μ M), and the role of PKC activity was assessed by pharmacological activation by phorbol 12-myristate 13-acetate (*PMA*) (10 ng/ml). Similar results were observed for SKOV3ip1 ovarian carcinoma cells (data not shown). Error bars represent S.E.

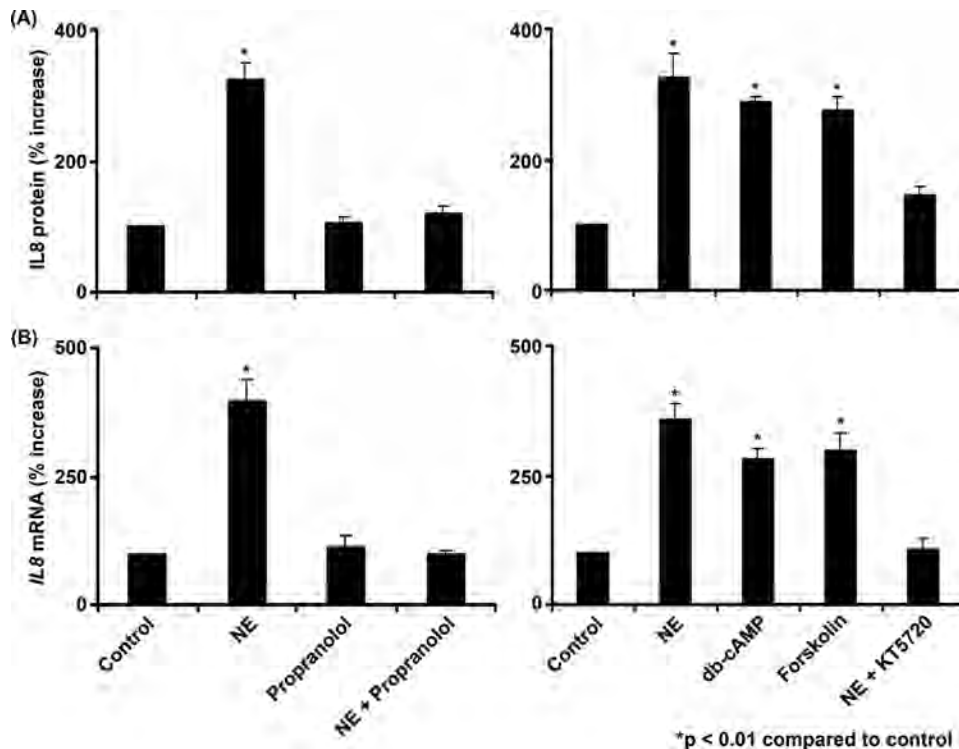


FIGURE 4. **Role of adrenergic signaling in IL8 expression.** IL8 expression was assessed in SKOV3ip1 ovarian cancer cells at protein (A) and mRNA levels (B) by ELISA and real time RT-PCR, respectively, after 6 h of exposure to NE (10 μ M). The role of β -adrenergic signaling was evaluated by pretreatment of NE-exposed cell with the β -blocker propranolol (10 μ M). The role of PKA activity was assessed by pharmacological activation by Bt₂cAMP (*db-cAMP*) (100 μ M) and forskolin (10 μ M). The importance of PKA in mediating NE-induced cellular responses was assessed by pretreatment of NE-exposed cells with a PKA-specific blocker KT5720. Similar results were observed for HeyA8 ovarian cancer cells (data not shown). Error bars represent S.E.

37 °C. Membranes were fixed, stained, and counted using light microscopy. Experiments were done in triplicate.

Assessment of Catecholamine Levels in Vivo—NE levels were quantified as described previously (1). Briefly, HPLC (Agilent 1100 binary HPLC) tandem mass spectrometry (Waters QuattroUltima, Waters) was used on frozen pulverized tumor tissues from stress *versus* nonstressed mice.

Short Interfering RNA (siRNA)—Twenty four hours prior to stimulation with NE or vehicle control, 1.0×10^6 SKOV3ip1 cells were transfected (HiPerfect, Qiagen) with siRNA to *Fos*, *FosB*, *Jun*, *JunB*, or negative control siRNA (Qiagen, Valencia, CA). Six hours later, cells were assayed for IL8 mRNA expression by real time pRT-PCR using established primer and probe sequences (Applied Biosystems, Foster City, CA). For *in vivo* studies, targeted siRNA, against human IL8 (target sequence, 5'-CAAGGAAGUGC AAAAGAA-3') and human FosB (target sequence, 5'-AGGUCACGUUGGCCCUCAA-3') were obtained from Sigma and incorporated into neutral nanoliposomes (1,2-dioleoyl-*sn*-glycero-3-phosphatidylcholine (DOPC), as described previously (28, 29).

Immunohistochemistry—After antigen retrieval or fixation, 3% H₂O₂ was used to block the endogenous peroxidase activity. Protein blocking of nonspecific epitopes was done using either 5% normal horse serum or 1% normal goat serum (IL8, Ki67, MMP-2, MMP-9, and CD31). Slides were next incubated with primary antibody to IL8 (rabbit polyclonal anti-human, 1:400 dilution; BIOSOURCE), Ki67 1:25 dilution, MMP-2 (rabbit polyclonal anti-human, 1:400 dilution; Chemicon, Temecula, CA), MMP-9 (rabbit polyclonal anti-human, 1:400 dilution; Chemicon), or CD31 (rat monoclonal anti-mouse, 1:800 dilution; Pharmingen) overnight at 4 °C. After washing with PBS, appropriate horseradish peroxidase-conjugated secondary antibody were added, and counter staining was done as described previously (1, 28). To quantify microvessel density (MVD), we examined 10 random 0.159-mm² fields at $\times 100$ magnification for each tumor and counted the microvessels within those fields (25).

Orthotopic Mouse Model of Chronic Stress—10–12-Week-old female athymic nude mice were obtained from the NCI-Frederick Cancer Research and Development Center (Frederick, MD) and housed in a pathogen-free environment. These mice were cared for according to the guidelines of the American Association for Accreditation and Laboratory Animal Care and the United States Public Health Service Policy on Human Care and Use of Laboratory Animals. All animal

work was approved by the MDACC Institutional Animal Care and Use Committee.

Mice were randomly assigned to one of the following six groups ($n = 10/\text{group}$): (a) control siRNA-DOPC; (b) *IL8* siRNA-DOPC; (c) FosB siRNA-DOPC; (d) control siRNA-DOPC + daily stress; (e) *IL8*-siRNA-DOPC + daily stress, and (f) FosB siRNA-DOPC + daily stress and appropriate groups were subjected to restraint stress for 3–4 weeks (HeyA8 and SKOV3ip1, respectively) as described previously (1). Briefly, human ovarian cancer cells (SKOV3ip1 and HeyA8) were grown in culture and collected (SKOV3ip1, trypsin in EDTA, or HeyA8, EDTA), washed with Hanks' balanced salt solution (Invitrogen), and resuspended at 1.25×10^6 cells per ml (HeyA8) or 5×10^6 cells per ml (SKOV3ip1); 200 μl of the appropriate cell suspension was injected in mice intraperitoneally. For metastasis-specific *in vivo* models, SKOV3ip1 (1.6×10^6) cells were suspended in 30 μl of Hanks' balanced salt solution (Invitrogen) and injected directly into the right ovary of anesthetized nude mice through a 1.5-cm intraperitoneal incision. One week after cell injection, staples were removed, and mice were subjected to daily restraint stress. siRNA-DOPC treatment directed against *IL8* or FosB was also started 7 days after tumor cell injection. Following tumor cell injection, restraint stress was continued for an additional 3 weeks. Targeted siRNA-DOPC therapy was continued twice weekly until the end of the experiment. At this point, mice were sacrificed; tumors were harvested, and the tumor weight and number and location of nodules were recorded.

For noninvasive imaging of metastasis and tumor growth *in vivo*, we used luciferase-expressing (30) SKOV3ip1 ovarian cancer cells (1×10^6). Mice were imaged by *in vivo* imaging system (Xenogen IVIS-200) weekly to assess tumor growth and metastasis.

Statistical Analysis—Continuous variables were compared with Student's *t* test if normally distributed. Differences in variables that were not normally distributed were compared using a nonparametric test (Mann-Whitney *U* test). Only two-tailed values are being reported in this study. We considered $p < 0.05$ to be significant.

RESULTS

Effect of NE Treatment on IL8 Production—We first examined whether NE or Epi stimulation directly increased IL8 production by ovarian cancer cells. IL8 levels were determined using ELISA (Fig. 1) and real time RT-PCR (Fig. 2). The mean basal level of IL-8 secretion by the ovarian cancer cells ranged between 78.4 and 182.7 pg/ml. NE treatment of ovarian cancer cells resulted in a 250–320% ($p < 0.01$) increase in IL8 protein (Fig. 1A). Epinephrine treatment resulted in similar increases (Fig. 1B) compared with control. Additionally, NE treatment resulted in a 240–320% ($p < 0.01$) increase in *IL8* mRNA levels compared with control (Fig. 2).

Role of NE in Transcriptional Control of IL8 Promoter—To determine whether increased transcriptional activity of the *IL8* promoter was responsible for catecholamine-mediated increases in *IL8* levels, we examined the effects of norepinephrine on a luciferase promoter construct driven by NE. Following transfection, HeyA8 ovarian cancer cells were assayed after 3 h

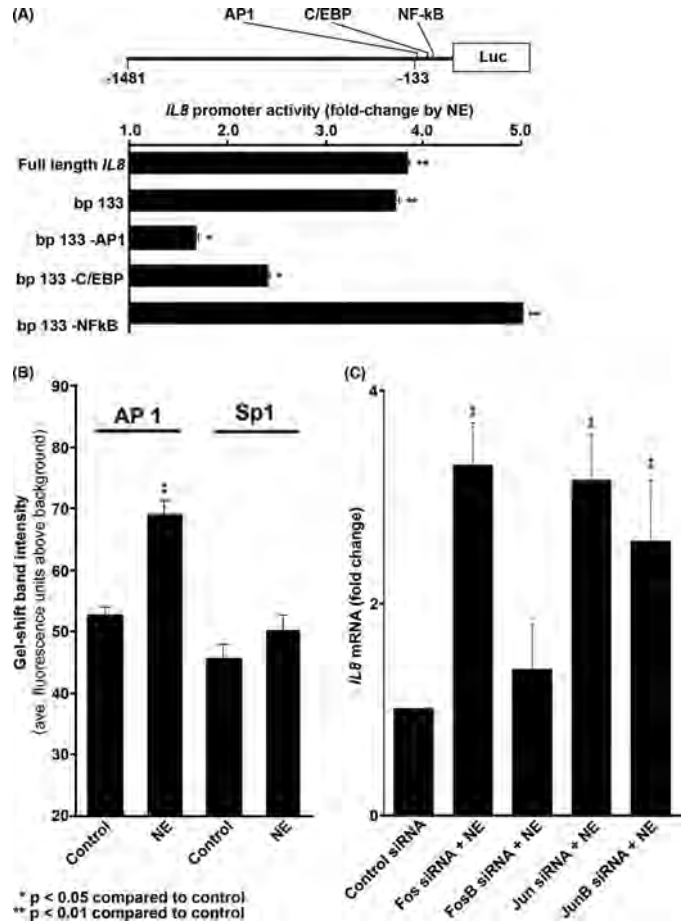


FIGURE 5. Role of AP1 in NE-mediated *IL8* induction. A, analysis of full-length and truncated *IL8* promoter sequences identified NE-responsive transcription elements within 133 bp upstream of the transcription start site. Site-directed mutagenesis of a predicted AP1 response element and a predicted CCAAT/enhancer-binding protein (C/EBP) (NFIL6) site each partially abrogated NE-mediated induction of the *IL8* promoter, whereas mutagenesis of a predicted NF- κ B response element enhanced *IL8* promoter response to NE. B, electrophoretic mobility shift assay of HeyA8 nuclear extracts using a fluorescence-tagged consensus oligonucleotide target to assess activation of AP1 or Sp1 15 min after exposure to NE. C, role of AP1 complex components in mediating NE-induced *IL8* expression was evaluated using real time RT-PCR in ovarian cancer cells after silencing Fos, FosB, Jun, and JunB. Average fold change in *IL8* mRNA is presented. Error bars represent S.E.

of exposure to norepinephrine (Fig. 3). Norepinephrine treatment resulted in 3.5–4-fold ($p < 0.05$) increase in *IL8* promoter activity. Pretreatment of ovarian cancer cells (HeyA8) with a β -blocker (propranolol) completely blocked the effects of NE. Direct activation of the β -adrenergically linked cAMP/PKA signaling pathway by Bt₂cAMP also resulted in 2.5-fold increase in *IL8* promoter activity ($p < 0.05$). Those effects were specific to the PKA pathway, as treatment with the PKC activator phorbol 12-myristate 13-acetate had no effect. Similar results were seen with the SKOV3ip1 cells (data not shown).

Role of Adrenergic Signaling in IL8 Production—Both ADRB1 and ADRB2 are expressed in the HeyA8 and SKOV3ip1 ovarian cancer cells (supplemental Fig. 1). To delineate the pathway responsible for increased IL8 levels, we determined the importance of ADRB in response to NE treatment (Fig. 4). IL8 protein (ELISA, Fig. 4A) and mRNA (real time RT-PCR, Fig. 4B) levels were assessed in the SKOV3ip1 ovarian cancer cells 6 h after exposure to NE. Treatment with NE resulted in 325% increase

IL8- and FosB-driven Tumor Growth

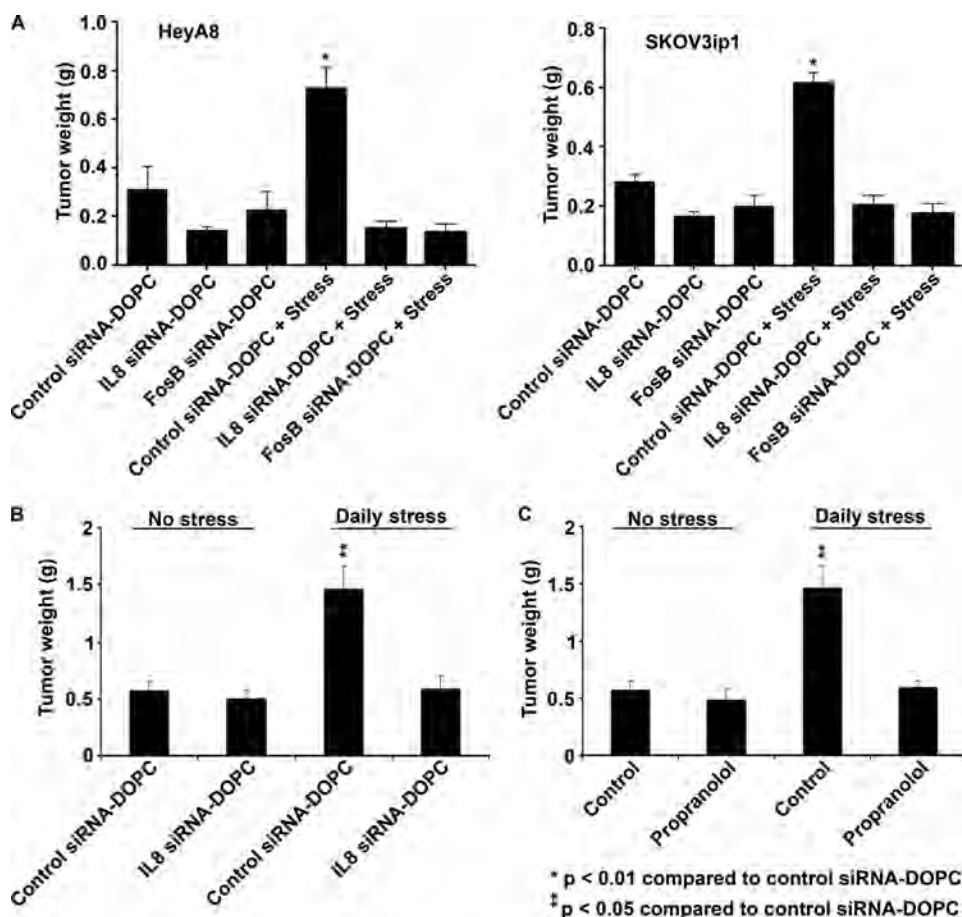


FIGURE 6. Effect of IL8 or FosB silencing on stress-mediated tumor growth. Nude mice were subjected to 2-h daily restraint stress each morning for 3–4 weeks using HeyA8 and SKOV31p1 ovarian cancer models. *A* and *B*, IL8 and FosB silencing was achieved with specific siRNAs incorporated into neutral nanoliposomal DOPC, injected twice weekly. *C*, ADRB activity was blocked with propranolol (β -blocker). At the end of each study, mice were sacrificed, and tumors were harvested. Average tumor weight (bar graph) is shown. Error bars, represent S.E.

in IL8 protein and 398% increase in IL8 mRNA levels compared with control ($p < 0.001$). In the absence of NE, propranolol (β -blocker) treatment alone had no significant effect on IL8 levels. Pretreatment of cells with propranolol completely abrogated the stimulatory effects of NE.

Next, the role of PKA was assessed (Fig. 4) by pharmacological activation by Bt_2cAMP or forskolin. Treatment of SKOV3ip1 cells with Bt_2cAMP or forskolin resulted in 282 and 298% increase in IL8 mRNA and 289 and 275% increase in IL8 protein levels ($p < 0.01$). The importance of PKA in mediating NE-induced cellular responses was further assessed by pretreatment of NE-exposed cells with a PKA-specific blocker (KT5720). Pretreatment of SKOV3ip1 cells with KT5720 completely abrogated NE-induced increases in IL8 mRNA and protein. Similar results were observed for HeyA8 cells (data not shown).

Determining the NE-responsive Transcriptional Elements—To identify the NE-responsive transcriptional elements, we utilized a truncated form of the IL8 promoter (Fig. 5A). The NE-responsive transcriptional elements were found within 133 bp upstream of the transcription start site. Here, NE signaling to a full-length IL8 promoter resulted in 3.8-fold induction ($p < 0.05$) in luciferase reporter gene activity. Site-directed

mutagenesis of predicted AP1 response elements and a predicted CCAAT/enhancer-binding protein (NFIL6) site each partially abrogated (by 55 and 39%, respectively) the NE-mediated induction of the IL8 promoter. Mutagenesis of a predicted NF- κ B response element enhanced IL8 promoter response to NE (by 31%, $p < 0.05$).

Next, we asked whether the AP1 complex was responsible for the catecholamine-mediated increases in IL8. To determine whether NE activated AP1 complex transcription factors, we assayed nuclear localization of AP1 (or Sp1 as a control) by electrophoretic mobility shift assay (EMSA) of nuclear proteins captured 15 min after NE exposure (Fig. 5B and supplemental Fig. 2). NE treatment resulted in a 50% greater band intensity ($p < 0.05$) compared with the control group. These effects were specific to AP1, in that NE had no significant effect on the magnitude of Sp1 binding.

We also performed an additional experiment to confirm our finding using an ELISA approach (supplemental Fig. 3). To determine the specific AP1 complex components responsive to NE treatment, we examined the NE-induced activa-

tion of specific AP1 family components (c-Fos, FosB, Fra1, c-Jun, JunB, and JunD) by detecting nuclear accumulation of individual proteins using ELISA. SKOV3ip1 cells exposed to NE (10 μ M) for 5 min resulted in the greatest increase in FosB protein (by 1.45-fold above base line).

Role of AP1 Complex Components in NE-induced IL8 Production—To identify the specific AP1 complex component responsible for catecholamine-mediated increase in IL8 levels, we assessed changes in IL8 mRNA with real time RT-PCR after silencing AP1 components (Fos, FosB, Jun, and JunB) with specific siRNAs followed by NE treatment (Fig. 5C). Despite Fos, Jun, and JunB silencing, NE treatment resulted in 2.5–3.3-fold increase in IL8 mRNA ($p < 0.01$). However, pretreatment of cells with FosB siRNA completely abrogated the stimulatory effects of NE.

Functional Effects of NE on Ovarian Cancer Cells—To determine whether NE promoted aggressive features in ovarian cancer cells, we carried out several experiments utilizing *in vitro* culture systems. First, we examined the effects of NE (10 μ M) on SKOV3ip1 cell proliferation at 48 h using Click-iT EdU Alexa Fluor-488 flow cytometry kit. NE treatment had no effect on ovarian cancer cell proliferation (supplemental Fig. 4A). Additionally, to determine whether catecholamine treatment

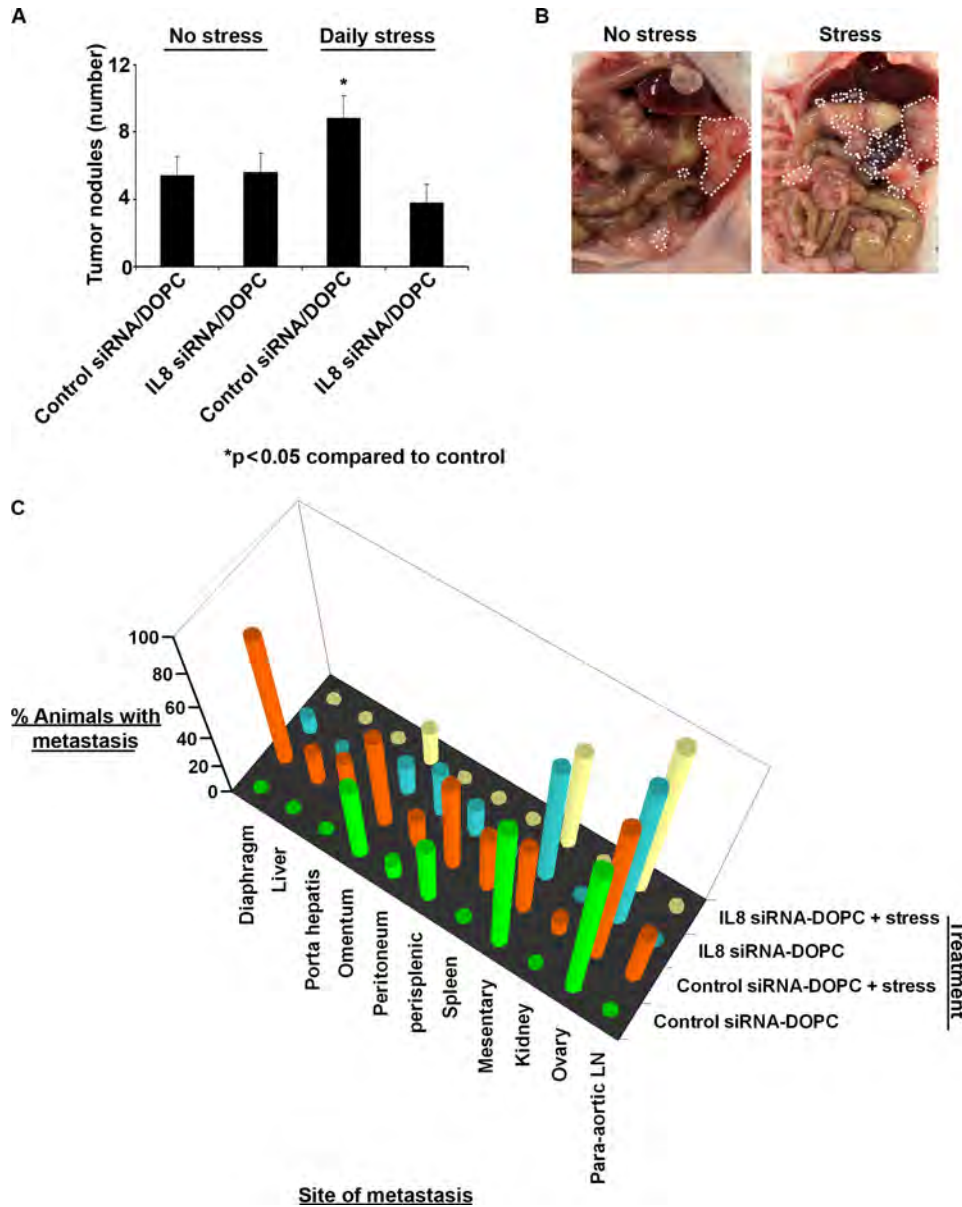


FIGURE 7. Effect of daily stress on patterns of metastasis. SKOV3ip1 cells were injected directly into the mouse ovary through a surgical skin incision. One week later, nude mice were subjected to a 2-h daily restraint stress each morning for 4 weeks. *A*, *IL8* silencing was achieved with specific siRNA incorporated into neutral nanoliposomal DOPC, injected twice weekly. At the end of the study, mice were sacrificed, and tumors were harvested. Average number tumor of nodules (*bar graph*) is shown. *Error bars* represent S.E. *B*, representative images of extent of metastatic spread in stress versus nonstress mice. Metastatic areas are outlined with *white dots*. *C*, *bar graph* represents percent of animals in each study arm with metastasis to intraperitoneal and distant organ sites. Para-aortic lymph nodes are depicted as *para-aortic LN*.

affected the cell cycle, we treated SKOV3ip1 cells for 6, 12, and 24 h with NE (10 μ M). NE treatment had no effect on cell cycle (*supplemental Fig. 4B*).

Next, to examine whether NE treatment affected tumor cell invasive and migratory potential and whether these effects were mediated via *IL8*, we used the membrane invasion culture system. The SKOV3ip1 cells were exposed to NE (10 μ M) with or without *IL8* siRNA. *IL8* siRNA without NE resulted in reduced invasion by 22% ($p < 0.05$) and migration by 38% ($p < 0.05$) compared with control siRNA treatment (*supplemental Fig. 4C*). NE treatment resulted in significantly higher invasion (60%, $p < 0.01$) and migration (128%, $p < 0.01$) compared with

controls. *IL8* siRNA abrogated the effects of NE on invasion and migration.

Effect of IL8 or FosB Silencing on Stress-mediated Tumor Growth and Metastasis—Based on our *in vitro* studies, we utilized a well characterized *in vivo* model of chronic stress to determine the biological relevance of *IL8* and *FosB*. We have recently shown that chronic stress leads to SNS activation and increased levels of NE/Epi, resulting in enhanced tumor growth and metastasis (1). We have also introduced a novel and effective method for *in vivo* siRNA delivery using DOPC nanoliposomes (29). In the stress group, mice were subjected to daily restraint stress for 2 h, which resulted in substantial increases in tumoral NE levels (65.9 pg/mg in controls versus 614.25 pg/mg in the stress group; $p < 0.001$). Daily restraint stress increased tumor growth by 235% (HeyA8, $p < 0.008$) and 221% (SKOV3ip1, $p < 0.001$; Fig. 6 and *supplemental Fig. 5*). *IL8* and *FosB* siRNA-DOPC in the non-stress setting resulted in reduced tumor weight (Fig. 6) in the HeyA8 (by 54%, $p = 0.18$, and 26%, $p < 0.5$, respectively) and SKOV3ip1 (by 41%, $p < 0.006$, and 28%, $p < 0.10$) models. *IL8* and *FosB* siRNA-DOPC completely blocked the stress-stimulated tumor growth in both animal models.

To address possible involvement of *IL8* and *FosB* in stress-mediated effects of metastasis, we also examined the number of nodules. In the nonstress setting, *IL8* and *FosB* siRNA-DOPC reduced the number of tumor nodules in both HeyA8 (by 40%, $p < 0.30$, and 42%, $p < 0.27$, respectively) and SKOV3ip1 (by 21%, $p < 0.30$, 51%, $p < 0.01$, respectively) models (*supplemental Fig. 6*). Tumor nodule counts in the control siRNA-DOPC + daily stress group were significantly higher (SKOV3ip1; 54%, $p < 0.01$). In the setting of chronic restraint stress, *IL8* and *FosB* siRNA completely abrogated the effects of stress on tumor metastasis.

Next, to determine the effects of daily restraint stress on the patterns of metastasis, we utilized a fully orthotopic mouse model whereby the tumor cells are injected directly into the ovary (31). SKOV3ip1 ovarian cancer cells were injected directly into the right ovary of nude mice followed

IL8- and FosB-driven Tumor Growth

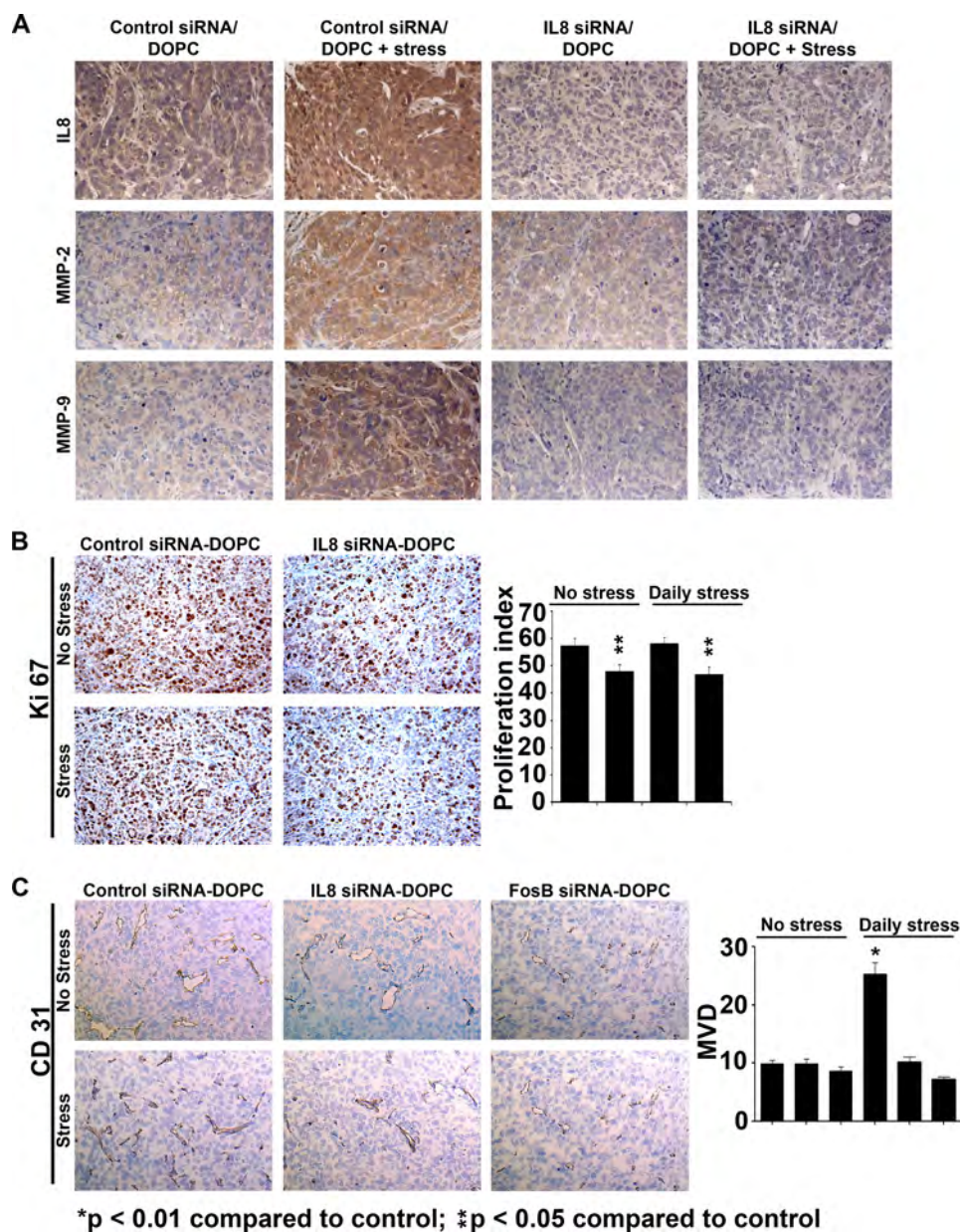


FIGURE 8. Effect of IL8 silencing on tumor microenvironment. *A*, immunohistochemical staining analysis of IL8, MMP-2, and MMP-9 expression in SKOV3ip1 tumors harvested from the chronic stress ovarian cancer model described in Fig. 6. Representative images (original magnification $\times 200$) are shown as follows: nuclei (blue) and IL8, MMP-2, and MMP-9 (brown). Tumor cell proliferation (*B*) and angiogenesis (*C*) was assessed by immunohistochemical staining for Ki 67 and CD31 antigens in tumors harvested at the end of *in vivo* experiments from all treatment groups. Representative photomicrographs representing Ki 67 (proliferative nuclei are brown; nonproliferative tumor cell nuclei are blue) and CD31 (mouse endothelial cells are blue; tumor cell nuclei are blue) staining (original magnification $\times 100$) are shown. The graph on the right shows proliferative index and mean number of MVD from each treatment group. Average MVD was calculated by averaging MVD counts from five random fields per slide, and at least three slides were examined for each treatment group. Error bars represent S.E.

by exposure to daily restraint stress, with or without *IL8* siRNA-DOPC treatment (Figs. 6*B* and 7*A*). In the nonstress setting, *IL8* siRNA-DOPC did not significantly affect metastasis. Daily restraint stress resulted in significantly higher (63%, $p < 0.04$) tumor nodule counts and distant metastatic spread compared with control siRNA-DOPC. *IL8* siRNA-DOPC completely abrogated the effects of stress on tumor metastasis. To confirm that metastatic nodules represented cancer tissue, we also utilized luciferase-labeled

SKOV3ip1 ovarian cancer cells (30) in this model and evaluated tumor growth and metastasis using weekly bioluminescence imaging (supplemental Fig. 8). Daily restraint stress resulted in substantially increased tumor growth and metastasis compared with controls.

To determine whether the effects of daily restraint stress were indeed due to mouse catecholamines, we used daily propranolol (β -blocker). In the nonstress setting, propranolol had no significant effect on tumor growth or metastasis. Chronic stress resulted in significantly higher tumor growth (156%, $p < 0.01$) and tumor metastasis (63%, $p < 0.04$). Concomitant treatment with propranolol abrogated the stimulatory effects of daily restraint stress (Fig. 6*C* and supplemental Fig. 7) on tumor growth.

Next, to determine the effect of chronic stress on IL8 protein levels, we used immunohistochemistry (Fig. 8*A*). Chronic stress resulted in substantially increased IL8 levels, whereas *IL8* siRNA-DOPC treatment effectively reduced IL8 expression in stress versus nonstress settings.

Role of IL8 in Mediating Stress-induced Changes in Tumor Microenvironment—To determine whether the tumor microenvironment played a role in stress-associated increases seen in tumor metastasis, we determined MMP-2 and MMP-9 levels in tumor tissues from the SKOV3ip1 orthotopic ovarian cancer metastasis model (Fig. 8*A*). Immunohistochemistry analysis revealed a substantial increase in MMP-2 and MMP-9 staining in tumors of mice that were exposed to daily restraint stress, which was

blocked by *IL8*-targeted siRNA.

To determine the effect of restraint stress on tumor cell proliferation, we stained (Ki 67) tumor tissues from stress versus nonstress mice that were treated with either nonspecific (control) siRNA or *IL8*-targeted siRNA (Fig. 8*B*). In the nonstress setting, *IL8* siRNA treatment resulted in 16% reduction ($p < 0.05$) in proliferation index compared with control. *IL8* siRNA in the stress groups resulted in 19% ($p < 0.05$) reduction in proliferation index. Daily stress had no effect on cell proliferation.

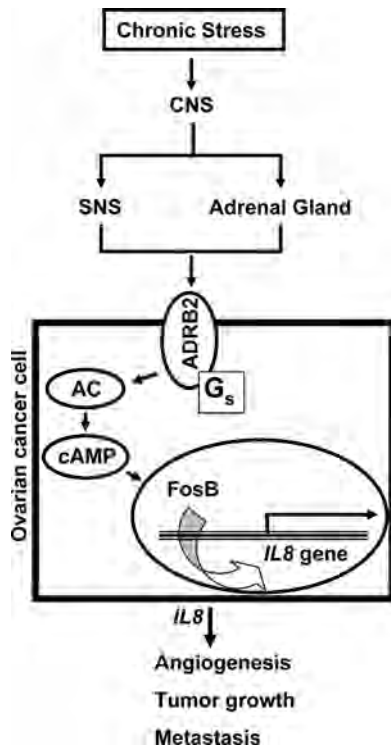


FIGURE 9. Role of IL8 and FosB in mediating the effects of chronic stress response on tumor growth. Chronic stress activates ADRB2 signaling, resulting in increased FosB and IL8 levels, which in turn promote tumor angiogenesis, growth, and metastasis. AC, adenylate cyclase.

Chronic stress is known to result in increased angiogenesis (1). Here, we asked whether IL8 and FosB mediated the effects of chronic stress on tumor angiogenesis (Fig. 8C). We assessed MVD on fresh frozen (OCT) tumor tissues from each of the six groups using CD31 staining. In the HeyA8 model, control siRNA-DOPC + daily stress resulted in significantly higher (157%, $p < 0.01$) MVD compared with the nonstress, control siRNA-DOPC treatment group. *IL8* or *FosB* siRNA-DOPC treatment resulted in complete abrogation of stress-induced angiogenesis and reduced the MVD count to that of the nonstress, control siRNA-DOPC treatment group. These findings further suggest that increased production of IL8 in response to chronic stress is mediated by FosB (Fig. 9). Here, elevated catecholamine levels first induce FosB followed by increased production of IL8, which consequently resulted in enhanced tumor growth and metastasis.

DISCUSSION

The key findings of this study are that the stress hormones NE and Epi can enhance IL8 expression and thereby mediate effects of stress on growth and metastasis of ovarian cancer. Our data also show that the AP1 complex component FosB plays a critical role in mediating these effects. This pathway proceeds through the ADRB2 and is blocked by propranolol. Furthermore, *in vivo* targeting of *IL8* and *FosB* with siRNA prevented stress-induced increases in tumor growth, metastasis, and tumor-associated angiogenesis. These effects appear to stem from a reduction in proangiogenic factors present in the tumor microenvironment that led to decreased tumor vascularity.

Many observations have suggested an association between chronic stress and malignant progression (32–34); however, there are little data elucidating the biological mechanisms of such effects. Most studies that link chronic stress to tumor progression have reported indirect effects such as via the immune system (32, 35). Chronic stress in both animals and humans has been shown to decrease cellular immune parameters (36–38). However, the uncertain role of immune system in solid tumors led us to consider an alternative hypothesis. Stress hormones from the SNS might directly regulate the growth and metastatic potential of tumor cells, and this effect might be independent of the immune system (1). Recent evidence confirms that alterations in neuroendocrine dynamics caused by chronic stress can directly regulate tumor pathogenesis (1, 2, 10, 39).

Chronic stress has been shown to increase NE and Epi levels leading to augmented tumor growth and metastasis (1). Once elevated, these catecholamines cause increased production of IL8, which is a potent proangiogenic cytokine overexpressed in most human cancers, including ovarian carcinoma (12–15). More recently, *IL8* gene silencing with liposomal siRNA incorporated in DOPC has shown decreased tumor growth and angiogenesis (24) in ovarian cancer.

FosB is a member of the *Fos* gene family (*Fos*, *FosB*, *FosL1*, and *FosL2*). Although this family of genes has been extensively studied as immediate early genes, the role of FosB in response to chronic stress has not been previously investigated. The Fos family of proteins form heterodimers with Jun family members and make up a variety of AP1 complexes. These AP1 complexes bind to the 12-*O*-tetradecanoylphorbol-13-acetate-response elements in the promoter and enhancer regions of their target genes (40), thus critically regulating many different cellular and biological processes (41). For instance, AP1-regulated genes include important regulators of cell survival, proliferation, invasion, metastasis, and angiogenesis (42–46). Δ FosB, which is a spliced variant of FosB, has been shown to mediate the effect of cocaine addiction in the nucleus accumbens, thereby contributing to cocaine addiction. Mice lacking full-length FosB express a specific behavioral defect in reproduction and do not have the ability to nurture their young (47). Our data indicate that FosB also plays a major role in IL8 induction in response to stress hormones.

IL8 has been shown to modulate matrix metalloproteinase expression in tumor and endothelial cells, thereby regulating angiogenic activity (22, 40, 48, 49). In this study, we show that NE treatment resulted in significantly increased *IL8* mRNA and protein levels. Our *in vitro* data indicate that *IL8* promoter activity is increased with NE and Epi treatment of ovarian cancer cells. This activity was abrogated with a β -blocker. *IL8* promoter deletion constructs identified the AP1 transcriptional complex as a potential mediator of these effects, and siRNA inhibition studies confirmed that FosB in particular mediates the effects of stress hormones, resulting in increased production of IL8. High levels of IL8, as demonstrated with our *in vivo* orthotopic mouse model, resulted in enhanced tumor growth and metastases. These stress-induced increases in tumor growth and metastasis were blocked by silencing *IL8* and *FosB* RNA. Moreover, the increased tumor growth and metastases seen in the control siRNA-DOPC + daily stress group com-

IL8- and FosB-driven Tumor Growth

pared with the nonstress control siRNA-DOPC group correlate with the effects of stress on angiogenesis. *IL8* and *FosB* silencing block the effects of stress-induced increases in tumor vascularity. These findings point to a prominent role for increased SNS activity in promoting tumor growth and metastasis via FosB-mediated production of IL8.

Although it has been known that biobehavioral processes modulate the activity of many hormones by the central nervous system (50, 51), and those processes in turn can modulate tumor cell biology (52, 53), specific interventions targeting the pathways involved in neuroendocrine function may represent novel strategies for helping individuals fight the effects of stress on tumor progression.

REFERENCES

1. Thaker, P. H., Han, L. Y., Kamat, A. A., Arevalo, J. M., Takahashi, R., Lu, C., Jennings, N. B., Armaiz-Pena, G., Bankson, J. A., Ravoori, M., Merritt, W. M., Lin, Y. G., Mangala, L. S., Kim, T. J., Coleman, R. L., Landen, C. N., Li, Y., Felix, E., Sanguino, A. M., Newman, R. A., Lloyd, M., Gershenson, D. M., Kundra, V., Lopez-Berestein, G., Lutgendorf, S. K., Cole, S. W., and Sood, A. K. (2006) *Nat. Med.* **12**, 939–944
2. Badino, G. R., Novelli, A., Girardi, C., and Di Carlo, F. (1996) *Pharmacol. Res.* **33**, 255–260
3. Vandewalle, B., Revillion, F., and Lefebvre, J. (1990) *J. Cancer Res. Clin. Oncol.* **116**, 303–306
4. Marchetti, B., Spinola, P. G., Pelletier, G., and Labrie, F. (1991) *J. Steroid Biochem. Mol. Biol.* **38**, 307–320
5. Rangarajan, S., Enserink, J. M., Kuiperij, H. B., de Rooij, J., Price, L. S., Schwede, F., and Bos, J. L. (2003) *J. Cell Biol.* **160**, 487–493
6. Enserink, J. M., Price, L. S., Methi, T., Mahic, M., Sonnenberg, A., Bos, J. L., and Taskén, K. (2004) *J. Biol. Chem.* **279**, 44889–44896
7. Drell, T. L., 4th., Joseph, J., Lang, K., Niggemann, B., Zaenker, K. S., and Entschladen, F. (2003) *Breast Cancer Res. Treat.* **80**, 63–70
8. Lang, K., Drell, T. L., 4th., Lindecke, A., Niggemann, B., Kaltschmidt, C., Zaenker, K. S., and Entschladen, F. (2004) *Int. J. Cancer* **112**, 231–238
9. Masur, K., Niggemann, B., Zanker, K. S., and Entschladen, F. (2001) *Cancer Res.* **61**, 2866–2869
10. Sood, A. K., Bhatti, R., Kamat, A. A., Landen, C. N., Han, L., Thaker, P. H., Li, Y., Gershenson, D. M., Lutgendorf, S., and Cole, S. W. (2006) *Clin. Cancer Res.* **12**, 369–375
11. Lutgendorf, S. K., DeGeest, K., Sung, C. Y., Arevalo, J. M., Penedo, F., Lucci, J., 3rd, Goodheart, M., Lubaroff, D., Farley, D. M., Sood, A. K., and Cole, S. W. (2009) *Brain Behav. Immun.* **23**, 176–183
12. Kassim, S. K., El-Salahy, E. M., Fayed, S. T., Helal, S. A., Helal, T., Azzam, Eel-D., and Khalifa, A. (2004) *Clin. Biochem.* **37**, 363–369
13. Koch, A. E., Polverini, P. J., Kunkel, S. L., Harlow, L. A., DiPietro, L. A., Elnor, V. M., Elnor, S. G., and Strieter, R. M. (1992) *Science* **258**, 1798–1801
14. Lokshin, A. E., Winans, M., Landsittel, D., Marrangoni, A. M., Velikokhatnaya, L., Modugno, F., Nolen, B. M., and Gorelik, E. (2006) *Gynecol. Oncol.* **102**, 244–251
15. Xie, K. (2001) *Cytokine Growth Factor Rev.* **12**, 375–391
16. Fidler, I. J. (2001) *J. Natl. Cancer Inst. Monogr.* **28**, 10–14
17. Folkman, J. (2002) *Semin. Oncol.* **29**, 15–18
18. Lutgendorf, S. K., Cole, S., Costanzo, E., Bradley, S., Coffin, J., Jabbari, S., Rainwater, K., Ritchie, J. M., Yang, M., and Sood, A. K. (2003) *Clin. Cancer Res.* **9**, 4514–4521
19. Karashima, T., Sweeney, P., Kamat, A., Huang, S., Kim, S. J., Bar-Eli, M., McConkey, D. J., and Dinney, C. P. (2003) *Clin. Cancer Res.* **9**, 2786–2797
20. Kim, S. J., Uehara, H., Karashima, T., McCarty, M., Shih, N., and Fidler, I. J. (2001) *Neoplasia* **3**, 33–42
21. Li, A., Varney, M. L., Valasek, J., Godfrey, M., Dave, B. J., and Singh, R. K. (2005) *Angiogenesis* **8**, 63–71
22. Luca, M., Huang, S., Gershenwald, J. E., Singh, R. K., Reich, R., and Bar-Eli, M. (1997) *Am. J. Pathol.* **151**, 1105–1113
23. Xu, L., and Fidler, I. J. (2000) *Oncol. Res.* **12**, 97–106
24. Merritt, W. M., Lin, Y. G., Spannuth, W. A., Fletcher, M. S., Kamat, A. A., Han, L. Y., Landen, C. N., Jennings, N., De Geest, K., Langley, R. R., Vilares, G., Sanguino, A., Lutgendorf, S. K., Lopez-Berestein, G., Bar-Eli, M. M., and Sood, A. K. (2008) *J. Natl. Cancer Inst.* **100**, 359–372
25. Thaker, P. H., Yazici, S., Nilsson, M. B., Yokoi, K., Tsan, R. Z., He, J., Kim, S. J., Fidler, I. J., and Sood, A. K. (2005) *Clin. Cancer Res.* **11**, 4923–4933
26. Mourad-Zeidan, A. A., Melnikova, V. O., Wang, H., Raz, A., and Bar-Eli, M. (2008) *Am. J. Pathol.* **173**, 1839–1852
27. Lev, D. C., Ruiz, M., Mills, L., McGary, E. C., Price, J. E., and Bar-Eli, M. (2003) *Mol. Cancer Ther.* **2**, 753–763
28. Halder, J., Kamat, A. A., Landen, C. N., Jr., Han, L. Y., Lutgendorf, S. K., Lin, Y. G., Merritt, W. M., Jennings, N. B., Chavez-Reyes, A., Coleman, R. L., Gershenson, D. M., Schmandt, R., Cole, S. W., Lopez-Berestein, G., and Sood, A. K. (2006) *Clin. Cancer Res.* **12**, 4916–4924
29. Landen, C. N., Jr., Chavez-Reyes, A., Bucana, C., Schmandt, R., Deavers, M. T., Lopez-Berestein, G., and Sood, A. K. (2005) *Cancer Res.* **65**, 6910–6918
30. Lee, J. W., Han, H. D., Shahzad, M. M., Kim, S. W., Mangala, L. S., Nick, A. M., Lu, C., Langley, R. R., Schmandt, R., Kim, H. S., Mao, S., Gooya, J., Fazenbaker, C., Jackson, D., Tice, D. A., Landen, C. N., Coleman, R. L., and Sood, A. K. (2009) *J. Natl. Cancer Inst.* **101**, 1193–1205
31. Lu, C., Thaker, P. H., Lin, Y. G., Spannuth, W., Landen, C. N., Merritt, W. M., Jennings, N. B., Langley, R. R., Gershenson, D. M., Yancopoulos, G. D., Ellis, L. M., Jaffe, R. B., Coleman, R. L., and Sood, A. K. (2008) *Am. J. Obstet. Gynecol.* **198**, 477.e1–10
32. Andersen, B. L., Farrar, W. B., Golden-Kreutz, D. M., Glaser, R., Emery, C. F., Crespino, T. R., Shapiro, C. L., and Carson, W. E., 3rd. (2004) *J. Clin. Oncol.* **22**, 3570–3580
33. Fawzy, F. I., Canada, A. L., and Fawzy, N. W. (2003) *Arch. Gen. Psychiatry* **60**, 100–103
34. Spiegel, D. (2002) *Nat. Rev. Cancer* **2**, 383–389
35. Andersen, B. L., Farrar, W. B., Golden-Kreutz, D., Kutz, L. A., MacCallum, R., Courtney, M. E., and Glaser, R. (1998) *J. Natl. Cancer Inst.* **90**, 30–36
36. Glaser, R., MacCallum, R. C., Laskowski, B. F., Malarkey, W. B., Sheridan, J. F., and Kiecolt-Glaser, J. K. (2001) *J. Gerontol. A Biol. Sci. Med. Sci.* **56**, M477–M482
37. Lutgendorf, S. K., Sood, A. K., Anderson, B., McGinn, S., Maseri, H., Dao, M., Sorosky, J. I., De Geest, K., Ritchie, J., and Lubaroff, D. M. (2005) *J. Clin. Oncol.* **23**, 7105–7113
38. Page, G. G., and Ben-Eliyahu, S. (1999) *Dev. Comp. Immunol.* **23**, 87–96
39. Palm, D., Lang, K., Niggemann, B., Drell, T. L., 4th., Masur, K., Zaenker, K. S., and Entschladen, F. (2006) *Int. J. Cancer* **118**, 2744–2749
40. Lamph, W. W., Wamsley, P., Sassone-Corsi, P., and Verma, I. M. (1988) *Nature* **334**, 629–631
41. Angel, P., and Karin, M. (1991) *Biochim. Biophys. Acta* **1072**, 129–157
42. Jochum, W., Passequé, E., and Wagner, E. F. (2001) *Oncogene* **20**, 2401–2412
43. Shaulian, E., and Karin, M. (2001) *Oncogene* **20**, 2390–2400
44. Shaulian, E., and Karin, M. (2002) *Nat. Cell Biol.* **4**, E131–136
45. Tulchinsky, E. (2000) *Histol. Histopathol.* **15**, 921–928
46. van Dam, H., and Castellazzi, M. (2001) *Oncogene* **20**, 2453–2464
47. Brown, J. R., Ye, H., Bronson, R. T., Dikkes, P., and Greenberg, M. E. (1996) *Cell* **86**, 297–309
48. Li, A., Dubey, S., Varney, M. L., Dave, B. J., and Singh, R. K. (2003) *J. Immunol.* **170**, 3369–3376
49. Yoneda, J., Kuniyasu, H., Crispens, M. A., Price, J. E., Bucana, C. D., and Fidler, I. J. (1998) *J. Natl. Cancer Inst.* **90**, 447–454
50. Antoni, M. H., Cruess, S., Cruess, D. G., Kumar, M., Lutgendorf, S., Ironson, G., Dettmer, E., Williams, J., Klimas, N., Fletcher, M. A., and Schneiderman, N. (2000) *Ann. Behav. Med.* **22**, 29–37
51. Turner-Cobb, J. M., Sephton, S. E., Koopman, C., Blake-Mortimer, J., and Spiegel, D. (2000) *Psychosom. Med.* **62**, 337–345
52. Costanzo, E. S., Lutgendorf, S. K., Sood, A. K., Anderson, B., Sorosky, J., and Lubaroff, D. M. (2005) *Cancer* **104**, 305–313
53. Lutgendorf, S. K., Anderson, B., Ullrich, P., Johnsen, E. L., Buller, R. E., Sood, A. K., Sorosky, J. I., and Ritchie, J. (2002) *Cancer* **94**, 131–140